


Experimental study on surface arc plasma actuation-based hypersonic boundary layer transition flow control

Hesen YANG (杨鹤森)¹ , Hua LIANG (梁华)^{1,*}, Shanguang GUO (郭善广)¹, Yanhao LUO (罗彦浩)¹, Mengxiao TANG (唐孟潇)¹, Chuanbiao ZHANG (张传标)¹, Yun WU (吴云)^{1,2,*} and Yinghong LI (李应红)^{1,2}

¹ Science and Technology on Plasma Dynamics Laboratory, Air Force Engineering University, Xi'an 710038, People's Republic of China

² School of Mechanical Engineering, Xi'an Jiaotong University, Xi'an 710048, People's Republic of China

E-mail: lianghua82702@163.com and wuyun1223@126.com

Received 5 March 2022, revised 26 April 2022

Accepted for publication 5 May 2022

Published 20 July 2022



CrossMark

Abstract

Effective control of hypersonic transition is essential. In order to avoid affecting the structural profile of the aircraft, as well as reducing power consumption and electromagnetic interference, a low-frequency surface arc plasma disturbance experiment to promote hypersonic transition was carried out in the $\Phi 0.25$ m double-throat Ludwig tube wind tunnel at Huazhong University of Science and Technology. Contacting printed circuit board sensors and non-contact focused laser differential interferometry testing technology were used in combination. Experimental results showed that the low-frequency surface arc plasma actuation had obvious stimulation effects on the second-mode unstable wave and could promote boundary layer transition by changing the spectral characteristics of the second-mode unstable wave. At the same time, the plasma actuation could promote energy exchange between the second-mode unstable wave and other unstable waves. Finally, the corresponding control mechanism is discussed.

Keywords: plasma actuation, flow control, surface arc discharge, hypersonic boundary layer transition, experimental study

(Some figures may appear in colour only in the online journal)

1. Introduction

As one of the key issues in the design of hypersonic vehicles, hypersonic boundary layer transition control is always a research hotspot in the aerospace field [1–4]. The huge difference between the laminar and turbulent flow states caused by the boundary layer transition affects local aerodynamic and aerothermal performance, which seriously affects the performance of aircraft [5].

In the field of boundary layer transition control, the delay or promotion of transition have their own different backgrounds. The purpose of delaying transition is to reduce the friction and heat transfer on the surface of aircraft, protect the

thermal protection system of the aircraft and improve the economy and safety of the aircraft [6]. However, in propulsion systems, scramjet [7] is the best inspiratory power device used in hypersonic aircraft. It is hoped that intake air is in a turbulent state, so that fuel can be fully mixed and burned and propulsion efficiency can be improved. If the engine intake air does not turn into a turbulent state, it is necessary to manually force the transition to meet the requirements of engine start-up [8].

After decades of development, in response to the requirements of forcing transition, researchers have made great achievements in basic issue research and control mechanisms, including passive control methods such as rough elements [9–11] and vortex generators [12, 13], active control methods such as active blowing/suction control [14] and CO₂

* Authors to whom any correspondence should be addressed.

injection [15], and other methods. Furthermore, ramp-type rough element arrays have successfully achieved forced transition in precursor X-43A and X-51A flight tests [16]. However, inevitably, passive transition devices have the disadvantage of introducing extra drag under off-designed conditions.

With the rapid development of hypersonic aircraft, good flight performance under wide speed conditions has become the most urgent need. Most importantly, with the change of incoming flow state and passive control device parameters, some passive transition devices, including rough elements, delay the effects of transition in some combination of parameters, which is unwanted in terms of improving engine efficiency [17]. In active transition devices, the blowing/suction operating system is complex and expensive [18], and CO₂ injection is highly dependent on the air source, thus making it difficult to realise engineering applications [19].

Plasma active flow control technology has various advantages, including quick response, wide frequency band, no moving parts, low energy consumption and diversified layout. Meanwhile, it is easy to adjust actuation parameters and realise feedback control [20, 21], with the potential to control the boundary layer [22]. Studies on the combination of plasma and boundary layer transition appeared as early as 1983 [23]; at that time, glow discharge plasma actuation was introduced as a disturbance to explore the development of the boundary layer in supersonic and hypersonic flows [24, 25]. Later, Casper *et al* used pulsed glow discharge as a controlled disturbance in hypersonic wind tunnel experiments, aiming to investigate pressure fluctuation fields below turbulent points in hypersonic boundary layers [26]. In 2018, Yates *et al* achieved accelerated cross-flow transition in a Mach 6 static wind tunnel using a dielectric barrier discharge plasma actuation array on a 7° half-angle cone model [27]. However, relatively speaking, if an actuator's life is considered, the dielectric barrier discharge actuator is not promising with respect to the promoting-turbulence effects of the scramjet intake, and surface arc discharge may be more favourable. That is because in supersonic and hypersonic conditions, the heat flow on the surface of the aircraft changes dramatically, and wall ablation often occurs; the insulating medium of dielectric barrier discharge actuator is very vulnerable to damage.

In 2020, Li *et al* introduced high-frequency glow discharge (105 kHz) as an artificial disturbance in a hypersonic flat boundary layer. The simulation results indicated that glow discharge plasma disturbance has significant effects on the second-mode unstable wave and can effectively trigger boundary layer transition [28]. The purpose of the introduction of high-frequency artificial disturbance is to experimentally explore the nonlinear mechanism of second-mode and the first-mode waves in the transition process of the hypersonic plate boundary layer. The team also introduced the lower-frequency (17–39 kHz) artificial glow discharge disturbance, and found the harmonic relationship between the first-mode unstable wave and the second-mode unstable wave, and the phase-lock phenomenon between them [29].

It is obvious that the ability to generate controlled disturbances with adjustable frequencies makes glow discharge a popular method for adding artificial disturbance. Glow discharge is essentially a kind of plasma disturbance, and it reflects the advantage of the wide frequency band of plasma actuation, which also inspires us that plasma actuation can not only provide a controllable disturbance source in studies on the evolution of transition processes, but also serves as a direct means of controlling the transition acting on the boundary layer.

However, glow plasma discharge [30] is a discharge mode with weak intensity and very small current (generally 1–100 mA), thus resulting in limited aerodynamic effects and limited effective regulation results on the hypersonic boundary layer. As regards forced transition, it is difficult to achieve an effective turbulence capacity to ensure normal start-up of the hypersonic inlet. In addition, in practical applications, the high-frequency power supply is more complex and larger in volume and weight, so it causes acute problems such as electromagnetic interference and incompatibility, which may even affect the normal work of other systems of the aircraft. Moreover, from the perspective of energy and power supply design, it is difficult to achieve high-frequency and high-energy actuation. Increasing injection energy under high-frequency conditions will pay a greater price. Therefore, if lower-frequency excitation can also promote transition, the cost-effectiveness of plasma actuation will be improved.

At present, in the field of hypersonic boundary layer transition control, there are few related experimental studies on lower-frequency active flow control methods. In this paper, in a Mach 6 conventional noise wind tunnel, a low-frequency surface arc plasma actuation was applied to a 7° half-cone sharp cone and the effects of promoting transition were obtained, which could provide a new method for transition control.

2. Experimental methods and design

The experiment was conducted in the $\Phi 0.25$ m double-throat Ludwig tube wind tunnel at Huazhong University of Science and Technology. Detailed descriptions of wind tunnels can be found in [31].

A 7° half-angle cone with a blunt head of 50 μm and a length of 400 mm was selected. Five 132B38 printed circuit board (PCB) sensors were arranged at five flow direction positions, namely $x = 232.24$ mm, $x = 257.05$ mm, $x = 312.62$ mm, $x = 337.43$ mm and $x = 362.99$ mm, to describe the relative process of transition from the perspective of pressure pulsation. At the same time, focused laser differential interferometry (FLDI) was also used to capture the unstable waves in the hypersonic boundary layer from the perspective of spatial density fluctuations. Details of the FLDI test system are given in [32].

The actuator is located at $x = 141.05$ mm, and the metal electrode profile is consistent with the cone. The electrode generates arc plasma actuation through an AC millisecond power supply, and the detailed parameters of the power

Table 1. Main parameters of the incoming flow.

$Ma_\infty (U_\infty/C)$	$Re^{-1} (\rho U_\infty/\mu)$	$U_\infty (\text{m s}^{-1})$	$\rho (\text{kg m}^{-3})$	$P_0 (\text{MPa})$	$T_0 (\text{K})$	$P_S (\text{Pa})$	$T_S (\text{K})$	$\mu (\text{Pa s})$
6.0	7.283×10^6	884.22	0.029	0.71	443	449.687	54.024	0.3521×10^{-5}

Ma_∞ , C , Re^{-1} , U_∞ , ρ , P_0 , T_0 , P_S , T_S and μ stand for the free-stream Mach number, the velocity of sound, the unit Reynolds number, the free-stream velocity, the free-stream density, the total pressure, the total temperature, the static pressure, the static temperature and viscosity coefficient.

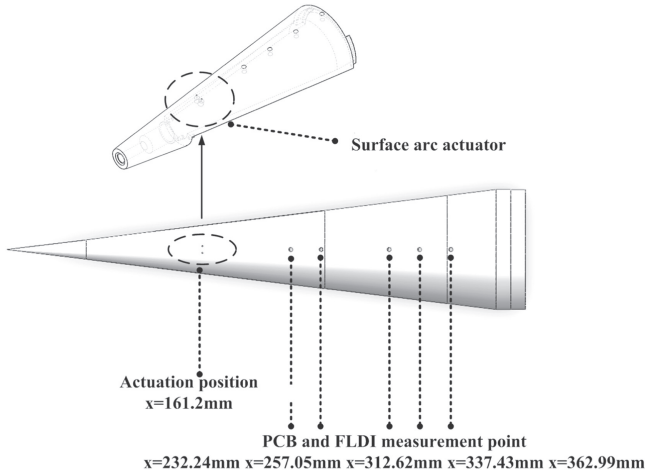


Figure 1. Surface arc actuator and measurement point distribution.

supply are described in [33]. The PCB sensor and actuator arrangement at the actuation position are displayed in figure 1.

3. Statement of results and analysis

Considering the disturbance mechanism and turbulence-promoting ability of surface arc actuation in supersonic flow [34], the expected transition position is located near the back of the model. By changing the total temperature and pressure of free incoming flow, $T_0 = 443 \text{ K}$, $P_0 = 0.71 \text{ MPa}$ and the unit Reynolds number $Re^{-1} = 7.283 \times 10^6 \text{ m}^{-1}$ are determined through repetitive experiments. The parameters of incoming flow are exhibited in table 1.

The PSD (power spectral density) of the PCB pressure sensor under this working condition is illustrated in figure 2. It is clear that the first four PCB pressure sensors along the flow direction all caught unstable waves, and the boundary layer on the cone surface is still a laminar flow. At $x = 232.24 \text{ mm}$, the unstable wave is obvious here. As the unstable wave develops along the flow direction to the point $x = 257.05 \text{ mm}$, the boundary layer gradually thickens and the unstable wave shows a left frequency shift; that is, the frequency shows a decreasing trend, but the amplitude of the unstable wave increases. According to the relationship between the wavelength of the second-mode unstable wave and the thickness of the boundary layer, the unstable wave can be basically determined as the second-mode unstable wave [35, 36].

When the flow reaches $x = 312.62 \text{ mm}$, the frequency of the second-mode unstable wave continues to decrease, and its

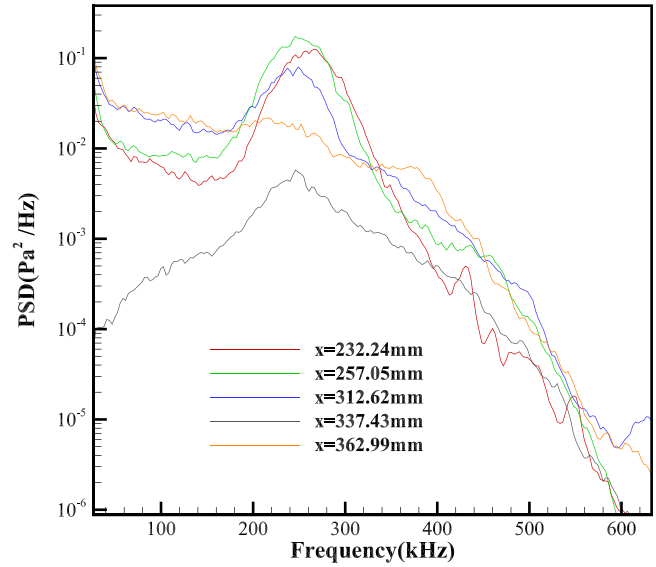


Figure 2. PSD of the PCB pressure sensors of base flow.

amplitude decreases slightly, but it still maintains the spectral characteristics of the second-mode unstable wave. On the other hand, when the flow continues to develop to $x = 337.43 \text{ mm}$, the spectral characteristics of the second-mode unstable wave gradually disappear, which means that the boundary layer is in the process of transition at this time. Furthermore, when the flow develops close to the tail end of the cone model ($x = 362.99 \text{ mm}$), the spectral characteristics of the second-mode unstable wave disappear completely, which indicates that the boundary layer flow at this point has become completely turbulent. Therefore, the transition position of base flow is located between the fourth and fifth PCB sensor positions.

In the same condition, the density pulsation at five PCB measuring points is measured by the FLDI system. When each flow direction position x is determined, the FLDI measuring point is located just above the surface of the cone without shading. The determination of the measuring point and its location diagram are shown in figure 3.

By analyzing the PSD of different flow direction positions measured by the FLDI system, it was found that the development and frequency shift trend of unstable waves along the flow direction are consistent with the results measured by the PCB sensor. As for the spectrum obtained by density pulsation analysis, it can also be judged that the transition region is located in the $x = 337.43\text{--}362.99 \text{ mm}$ region, which suggests that the FLDI system can successfully capture the second-mode unstable wave as a reliable means to study the hypersonic sharp cone boundary layer.

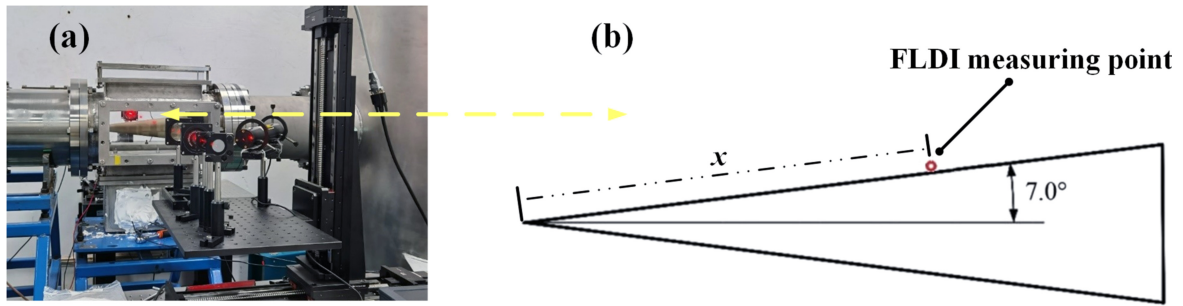


Figure 3. Determination of FLDI measuring point position and focus. (a) FLDI test system, (b) position of the FLDI measuring point.

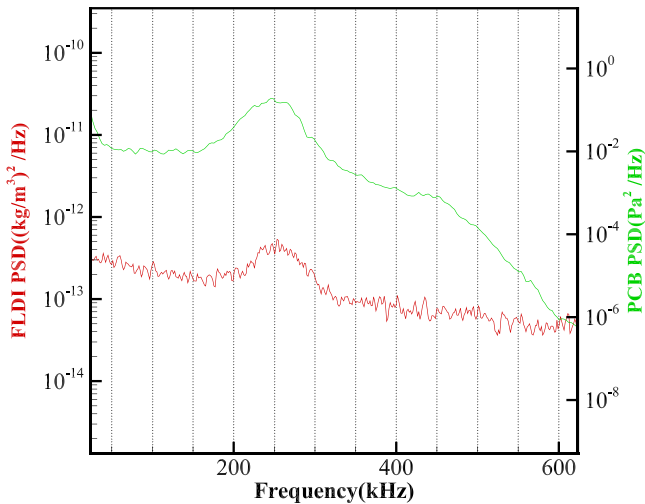


Figure 4. Comparison of FLDI and PCB spectra at $x = 257.05$ mm.

Through further analysis of frequency characteristics of the second-mode unstable wave, it is obvious that the frequency at the peak amplitudes collected by the FLDI system and the PCB sensor are the same, with a slight difference in the frequency bandwidth, which further demonstrates the reliability of the FLDI system. Figure 4 demonstrates the spectrum comparison of pulsation signals collected by the FLDI and PCB systems at a certain flow position.

After confirming the plasma discharge stability and its influence on the signal-to-noise ratio of the FLDI system under experimental incoming flow conditions, parameter combination of actuation voltage peak-to-peak value $V_{P-P} = 0.88$ kV and actuation frequency $f = 5.478$ kHz were determined. Stable discharge, a typical discharge waveform and the corresponding discharge circuit diagram are displayed in figure 5.

In order to obtain finer boundary layer transition control effects, seven flow directions along the flow direction ($x = 161.2$ mm, $x = 182.59$ mm, $x = 207.44$ mm, $x = 232.24$ mm, $x = 257.05$ mm, $x = 287.81$ mm and $x = 312.62$ mm) were selected. The power spectrum of the unstable wave at the corresponding wall surface was obtained through the FLDI system. The base flow was first measured at each position, followed by the measurement of the situation under actuation. The results are shown in figure 6.

After applying surface arc actuation, the spectral characteristics of the whole frequency band, especially those near

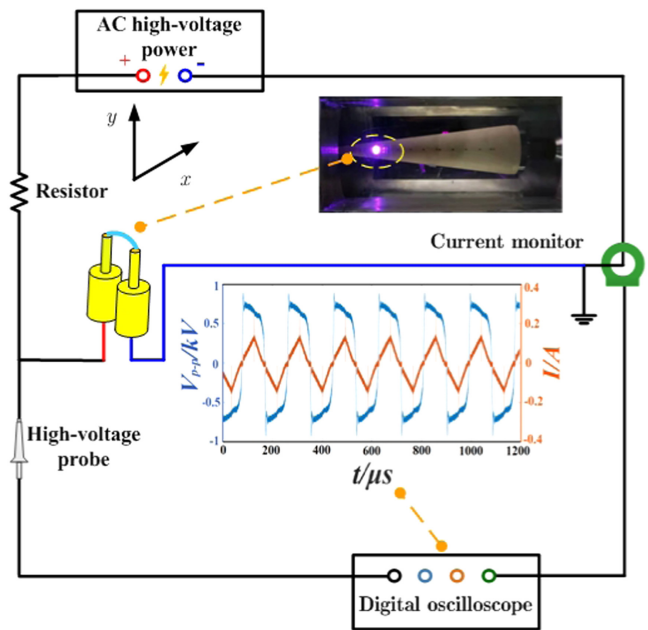


Figure 5. Discharge circuit diagram and a typical discharge waveform.

the low-frequency band and the second-mode unstable wave band, are significantly different. From $x = 161.2$ mm to $x = 182.59$ mm, the frequency spectrum under actuation reveals that the amplitude of the PSD in the whole frequency band increases and the second-mode unstable wave shifts slightly to the left, which indicates that the plasma actuation injects energy into the boundary layer and thickens the boundary layer. When the flow continues to develop to $x = 207.44$ mm and $x = 232.44$ mm, it can be observed that the actuation weakens the characteristics of the second-mode unstable wave, which suggests that the boundary layer transition has a tendency to happen earlier with plasma on.

However, in order to understand the influence of surface arc actuation on the boundary layer and the change of its development trend, the spectral characteristics at the actuation position are also very important. Therefore, two FLDI measurement points $x = 141.05$ mm (the actuation position) and $x = 151.13$ mm are added based on the measurement points selected in figure 7. The characteristics of hypersonic boundary layer controlled by surface arc actuation are

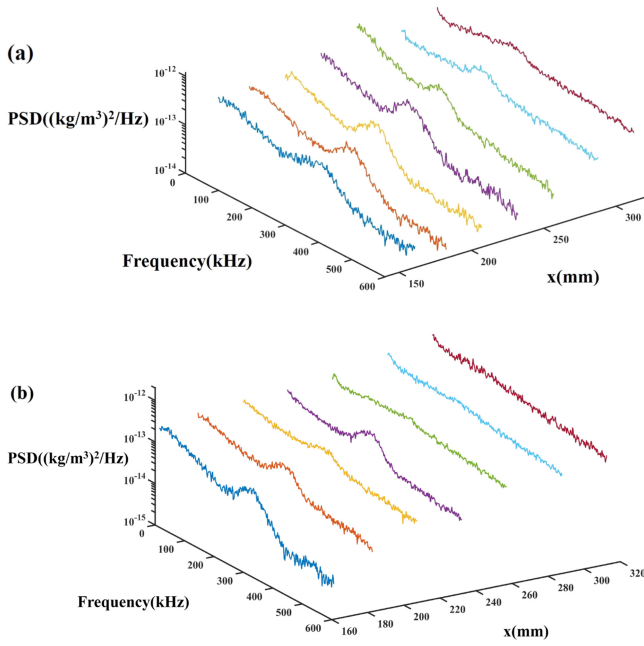


Figure 6. Distribution of the PSD of the second-mode unstable wave at different directions. (a) base, (b) actuation.

explored by analyzing the changes of the PSD characteristics of these nine flow positions.

Comparison of PSD before and after actuation at these nine positions is shown in figure 7. The key to obtaining the plasma actuation regulation effects and characteristics is to analyze its influence on the second-mode unstable wave, so only the PSD near the second-mode unstable wave band is selected for analysis.

Firstly, the position of the actuation location is considered. After surface arc actuation is applied, the most intuitive control effect is the increase of the amplitude of the frequency range studied, in which the PSD peak is increased by 17.57%, and the corresponding frequency of the peak is around 350 kHz. The increase of amplitude indicates that the surface arc actuation injects energy into the boundary layer, but the actuation does not change the spectral morphology of the second-mode unstable wave in this direction.

Analysis was continued along the flow direction, and the PSD results of flow direction position $x = 151.13$ mm are shown in figure 7(b). The results show that the increase of overall amplitude is still observed at this position, and the actuation still does not change the spectral morphology of the second-mode unstable wave. At the same time, it can be obviously found that under the action of surface arc actuation, the bandwidth of the second-mode unstable wave increases from 300 to 460 kHz under baseline to 282–450 kHz under actuation state. However, the actuation does not change the frequency corresponding to the peak PSD, which is around 340 kHz before and after actuation. Only the peak value of the PSD curve is increased, and the value is increased by 53.16% compared with baseline.

As the flow develops to flow direction $x = 161.2$ mm, it is found through spectrum analysis that the effect of surface

arc actuation at this flow direction position is similar to that at the first two flow direction positions, both of which show an increase in the overall amplitude, increase of the peak PSD and increase of the bandwidth while basically not changing the peak characteristic frequency. From the viewpoint of the first three positions, the characteristic frequency of the second-mode unstable wave moves to the left with the increase of the flow direction distance. Since the length of the second-mode unstable wave is about twice that of the thickness of the local boundary layer, the boundary layer thickness increases with the downstream development of the flow.

When the flow direction $x = 182.59$ mm, new actuation regulation characteristics appear. Under the control of surface arc actuation, the amplitude of the second-mode unstable wave is increased and its frequency range is shifted to the left. The characteristic frequency corresponding to the peak PSD is shifted to the left by 16 kHz; that is, the characteristic frequency is decreased by 5%. This indicates that the surface arc actuation not only injects energy to the boundary layer and promotes the growth of the second-mode unstable wave, but also thickens the boundary layer through the interaction between plasma actuation and the boundary layer at a certain flow distance. For the flow direction position $x = 207.44$ mm, the surface arc actuation achieves a similar control effect at the position $x = 182.59$ mm.

Moving further downstream, it is found that when the flow direction reaches $x = 232.24$ mm, the surface arc actuation changes the spectral morphology of the second-mode unstable wave and weakens the characteristics of the second-mode unstable wave. The PSD curve under actuation appears to have a ‘platform’ shape, but the amplitude of the second-mode unstable wave under actuation still increases compared to that of $x = 207.44$ mm.

When $x = 257.05$ mm, the spectral characteristics of the second-mode unstable wave almost disappear under the action of surface arc actuation. In terms of amplitude, the amplitude of the second-mode unstable wave is attenuated at this position compared with the position of $x = 232.24$ mm, indicating that a transition from laminar flow to turbulence is taking place in the boundary layer under actuation. At this time, the second-mode unstable wave of base flow is still in the stage of amplitude increasing, that is, a laminar flow state.

The flow continues to develop along the flow direction until $x = 287.81$ mm and $x = 312.62$ mm. PSD curves are shown in figures 7(h) and (i). It can be seen that, under actuation, the power spectrum of low-frequency disturbance increases and the level of turbulence in the boundary layer continues to improve. At this time, the amplitude of the second-mode unstable wave of base flow is still increasing and the base flow still does not transition.

In addition to the transverse comparison before and after actuation at each position, from the longitudinal comparison of the flow direction position, the amplitude of the base flow keeps increasing while the characteristic frequency keeps decreasing. The surface arc actuation does not change this trend, but the amplitude of the second-mode unstable wave is decreased at the earlier flow position, as seen in figure 8.

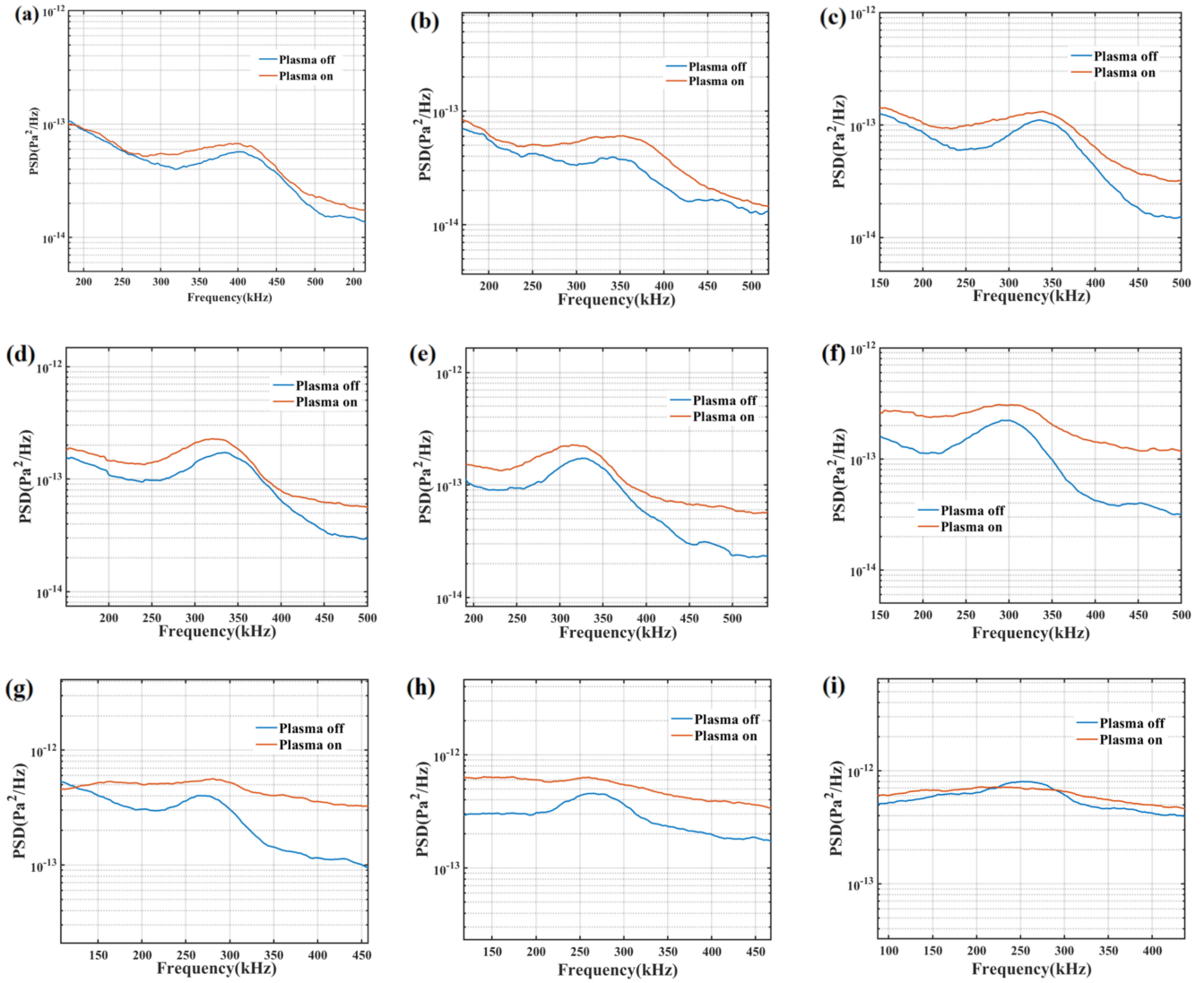


Figure 7. Comparison of the PSD of the second-mode unstable wave in different directions. (a) $x = 141.05$ mm, (b) $x = 151.13$ mm, (c) $x = 161.2$ mm, (d) $x = 182.59$ mm, (e) $x = 207.44$ mm, (f) $x = 232.24$ mm, (g) $x = 257.05$ mm, (h) $x = 287.81$ mm, (i) $x = 312.62$ mm.

There are several important stages in the transition process of the tip cone boundary layer. First, the amplitude of the second-mode unstable wave increases linearly for a long time, and then after a short nonlinear growth, it tends to be saturated and broken into isolated turbulent patches. Finally, the turbulent patches develop and fuse into complete turbulence. It can be concluded that surface arc actuation has the ability to regulate the hypersonic boundary layer and make the transition happen earlier.

In addition, although the surface arc actuation can lift the spectrum for each direction position, the PSD peak of the base flow is larger than that of actuation state in the whole direction position. This indicates that the surface arc actuation injects energy into the unstable waves in a wide frequency band in the boundary layer, and promotes the energy exchange and mixing between the second-mode and other unstable waves as well as the growth of the second-mode unstable wave.

According to the linear stability theory, the second-mode unstable wave can be further focused and its spatial growth rate can be calculated according to the test results of two adjacent FLDI measuring points to further verify the effect of surface arc actuation on the second-mode unstable wave. Figure 9 shows the corresponding growth rate results of the five flow direction positions, which are $x = 146.09$ mm, $x = 156.165$ mm, $x = 219.84$ mm, $x = 244.645$ mm and $x = 300.215$ mm.

Obviously, the surface arc actuation increases the growth rate of the unstable wave (including the second-mode unstable wave band) in a wide frequency range in the first three flow directions, which also indicates that the growth rate of the second-mode unstable wave is accelerated under actuation. At the fourth direction position $x = 244.645$ mm, the growth rate of the second-mode unstable wave spectrum corresponding to baseline is still maintained at a higher level, while the growth rate under actuation has dropped to a very

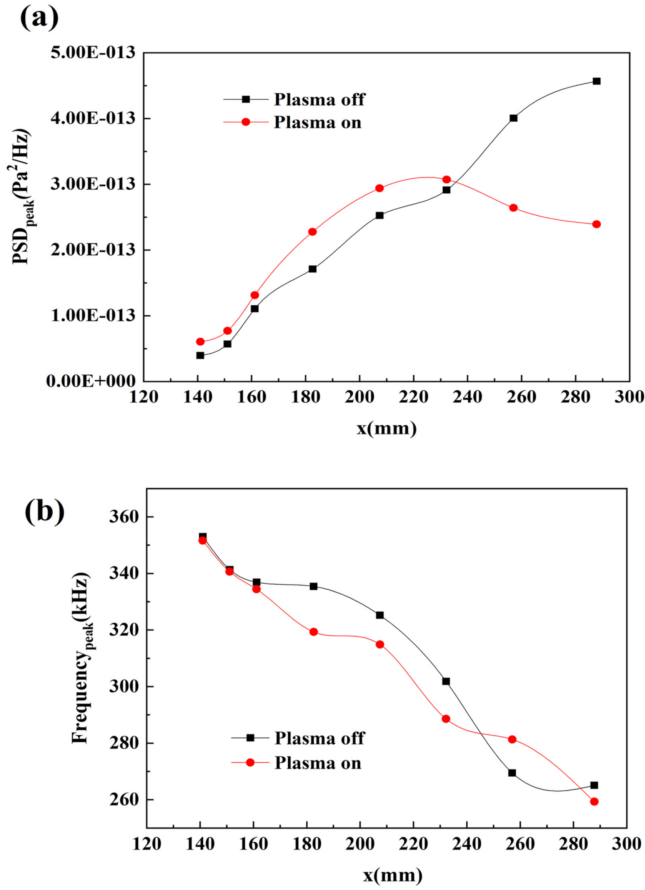


Figure 8. Comparison of PSD_{peak} and $\text{Frequency}_{\text{peak}}$ at different directions. (a) PSD_{peak} , (b) $\text{Frequency}_{\text{peak}}$.

low level; especially, the growth rate of the frequency band around the second-mode unstable wave characteristic frequency has shown negative growth, which indicates that the growth of the second-mode unstable wave has developed to saturation, and the flow at this position has entered the transition stage. As the flow continues to develop to $x = 300.215$ mm, the second-mode unstable wave of the baseline still keeps a steady growth, the flow still keeps laminar flow and the second-mode unstable wave under actuation has attenuated, which verifies that the second-mode unstable wave has made sufficient energy exchange with other unstable waves under actuation at this stage.

Hence, the low-frequency surface arc plasma actuation has obvious stimulation effects on the second-mode unstable wave, and the energy distribution of unstable waves in different frequency bands in the boundary layer is changed from the perspective of spatial growth rate. This makes the second-mode unstable wave grow and break in advance, which contributes to earlier transition.

4. Discussion of control mechanisms

At present, there are very few experimental studies on the control of the hypersonic boundary layer based on surface arc actuation, and analytical sensor data are few. In this research

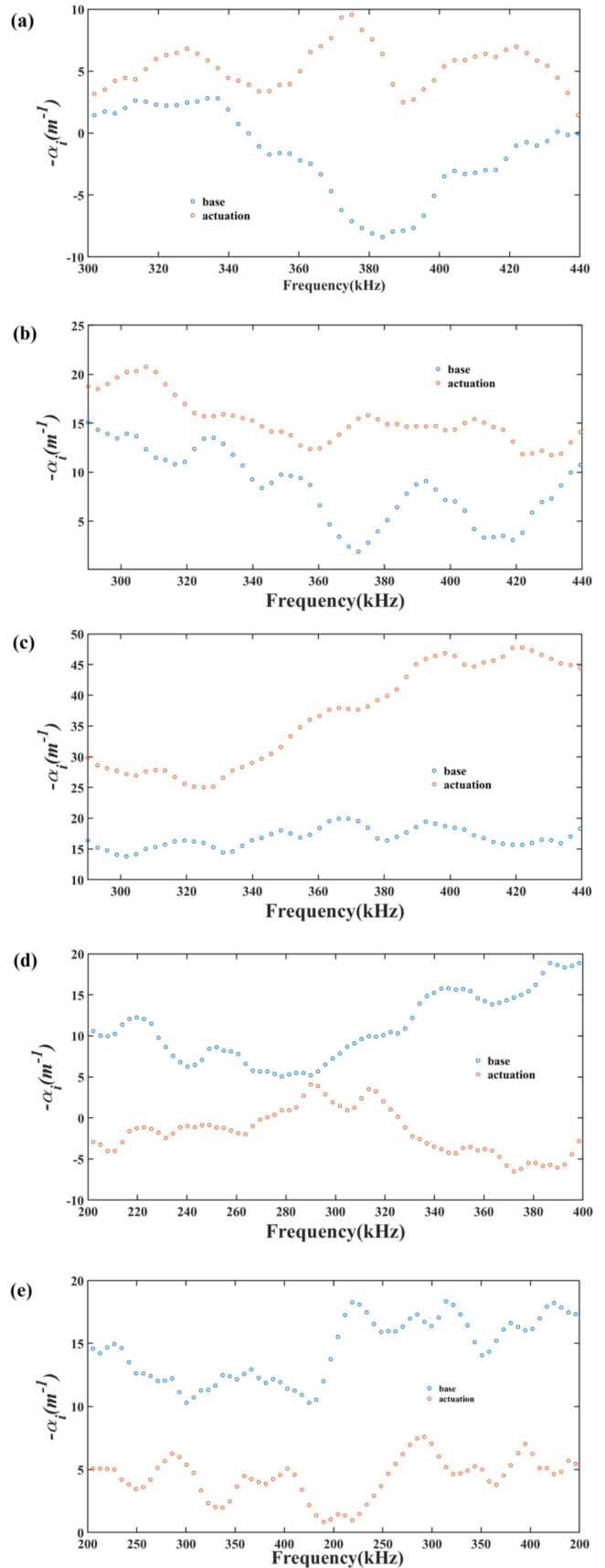


Figure 9. Spatial growth rate around the characteristic frequency of the second-mode unstable wave at different flow positions. (a) $x = 146.09$ mm, (b) $x = 156.165$ mm, (c) $x = 219.84$ mm, (d) $x = 244.645$ mm, (e) $x = 300.215$ mm.

respect, the application of flow display technology and corresponding numerical simulation work are also lacking. Therefore, it is difficult to intuitively obtain and summarize the internal control mechanism. However, we can carry out effective discussion and extraction based on the original understanding and consensus on the characteristics of the plasma actuator, the influence of some physical parameters on hypersonic boundary layer and the macro and micro combination of plasma generation, so as to guide the subsequent experimental research and simulation work.

The first is the shock wave effect (impact effect) [37]. Surface arc actuation can induce shock waves in supersonic and hypersonic flow fields. This is due to the temperature and pressure rise generated at the moment of breakdown, and the shock wave can produce coherent structure coupling with the supersonic/hypersonic boundary layer.

In the experimental study of promoting transition in supersonic flow, we have preliminarily revealed the mechanism combined with flow display technology. The core of the internal control mechanism is that the plasma actuation has the ability to induce an artificial hairpin vortex with the development of an induced shock wave. The hairpin vortex structure induced by surface arc actuation plays a crucial role in the process of promoting boundary layer transition. The conceptual model of hairpin vortex generation and evolution was proposed, which preliminarily revealed the physical process of the boundary layer transition promoted by surface arc actuation, which can be divided into three stages: generation and lifting of high vorticity region, formation of Λ vortex and evolution of hairpin vortex [38]. In the case of hypersonic flow, we will reveal this process by means of high-precision flow field display technology in a subsequent investigation.

The second is the thermal effect [39], the instantaneous temperature rise generated by surface arc actuation discharge will inevitably affect the unstable wave characteristics in the boundary layer. For the control mechanism, the heating effect causes changes of the boundary layer's thickness and the corresponding position of sound velocity line, which will lead to changes in velocity evolution of the disturbance wave phase in the boundary layer and migration of synchronous points, thus achieving the purpose of controlling transition [40, 41]. In the analysis of the spectral characteristics of the second-mode unstable wave in this work, it has been speculated that the hypersonic boundary layer thickens after a surface arc actuation is applied.

Surface arc actuation can quickly heat the boundary layer [38, 42]. According to verified results [43], the wall heating causes the boundary layer to be thick, and local heating makes the transition happen earlier. This seems to be a satisfactory trend, while the perturbation of the plasma to the boundary layer is by no means just a simple temperature change. Plasma is essentially a model of multi-physics coupling.

Finally, investigating the acoustic characteristics closely related to the second-mode unstable wave, such as discovering if whether AC surface arc actuation can induce acoustic disturbances [44, 45], may become the key to reveal the integrated mechanism of transition.

Based on the development of the current research on the characteristics of plasma actuators, combined with the unique physical properties in the hypersonic boundary layer [46], the authors deduced that the steady surface arc actuation used in the experiment described here can produce acoustic disturbance and it interacts with second-mode unstable waves.

This inference is based on two points. One is that the actuation used in this experiment is AC-steady actuation and AC-dielectric barrier discharge actuation has been experimentally confirmed and can produce acoustic disturbances [44]. The second is that the surface arc actuation of $f = 5.478$ kHz can generate high-amplitude current pulses, and the energy released by these current pulses will cause significant changes in the temperature and pressure of the gas near the actuator. In fact, arc discharge is essentially a process from glow discharge to spark discharge and finally arc discharge develops. The heat generated by glow discharge causes pressure changes near the surface of the plasma actuator, which is likely to form pressure oscillations and finally generate acoustic disturbance [47], thus creating conditions for the interaction between plasma actuation and the second-mode unstable wave, with essentially acoustic perturbation.

The three control mechanisms mentioned above must be coupled with each other in actual situations, which needs to be carefully studied in subsequent experiments.

5. Conclusion

Regarding the regulating effects of surface arc actuation on the hypersonic boundary layer, the characteristics of controlling the hypersonic boundary layer based on low-frequency surface arc actuation can be summarized as follows:

- (1) From the perspective of spectral characteristics, low-frequency surface arc actuation can promote boundary layer transition by changing the spectral characteristics of the second-mode unstable wave.
- (2) In terms of spatial growth rate, the low-frequency surface arc plasma actuation has an obvious stimulating effect on the second-mode unstable wave.
- (3) From the perspective of energy exchange, the low-frequency surface arc plasma actuation not only injects energy into the second-mode unstable wave, but also promotes energy exchange between the second-mode unstable wave and other unstable waves, and finally makes the second-mode unstable wave destabilize in advance.
- (4) The subsequent regulation of the internal physical control mechanism needs to start from the vortex structure induced by actuation, the heating effect and the acoustic disturbance induced by an AC plasma power supply, and the corresponding experimental research should be carried out in depth.

The last thing to note is that, limited by the experimental testing methods, the experimental work in this paper only corresponds to the development of the second-mode unstable wave and the transition process of the boundary layer, and

then the second-mode unstable wave induced by the plasma actuation is studied on this basis; hence, the ability of surface arc plasma actuation to induce transition is analyzed qualitatively through the development and change of the second-mode unstable wave. In addition, it cannot be denied that hypersonic transition is a complex process of multi-mode interaction. The second-mode unstable wave cannot always play a decisive and dominant role. The research on other modes, especially the first-mode wave, cannot be ignored under low-frequency actuation. Therefore, more research is needed to focus on the specific interactions between the second-mode unstable wave and other unstable waves, and more experimental comparisons between discharge and non-discharge conditions are also needed to verify the transition control capability dimension of plasma actuation and develop plasma actuation methods for transition control.

Acknowledgments

The work of this research is supported by National Science and Technology Major Project (No. J2019-II-0014-0035). Thanks to Associate Professor Wu Jie of Huazhong University of Science and Technology for the guidance of this experiment. Thanks to Sima Xuehao, Gui Yuteng and Huang Ranran for their help in the experiments.

ORCID iDs

Hesen YANG (杨鹤森)  <https://orcid.org/0000-0002-3391-6299>

References

- [1] Kimmel R 2003 Aspects of hypersonic boundary layer transition control *41st Aerospace Sciences Meeting and Exhibit* 2003, 772
- [2] Qi H et al 2021 *Adv. Aerodyn.* **3** 21
- [3] Middlebrooks J B et al 2021 Design of a hypersonic boundary layer transition control experiment utilizing a swept fin cone geometry in mach 6 flow *AIAA Scitech 2021 Forum* 2021 (AIAA) 1205 (<https://doi.org/10.2514/6.2021-1205>)
- [4] Yang H et al 2022 *Adv. Aerodyn.* **4** 1
- [5] Chen J Q et al 2021 *Appl. Therm. Eng.* **194** 116931
- [6] Fiévet R et al 2020 Numerical study of hypersonic boundary-layer transition delay through second-mode absorption *AIAA SciTech 2020 Forum (Orlando)* (AIAA)
- [7] Seleznev R K, Surzhikov S T and Shang J S 2019 *Prog. Aerosp. Sci.* **106** 43
- [8] Ding F et al 2018 *Acta Astronaut.* **152** 639
- [9] Reda D C, Wilder M C and Prabhu D K 2010 *J. Spacecraft Rockets* **47** 828
- [10] Tang X J et al 2021 *J. Phys. Conf. Ser.* **2012** 012027
- [11] Tang X J et al 2021 *J. Phys. Conf. Ser.* **1748** 052032
- [12] Estruch-Samper D et al 2015 *Shock Waves* **25** 521
- [13] Sun D et al 2020 *Phys. Fluids* **32** 126111
- [14] Demetriades A et al 2015 *J. Spacecraft Rockets* **13** 508
- [15] Miró F M and Pinna F 2020 *J. Fluid Mech.* **890** R4
- [16] Lau K Y 2008 *J. Spacecraft Rockets* **45** 176
- [17] Tang Q et al 2015 *Phys. Fluids* **27** 064105
- [18] Kornilov V I 2015 *Prog. Aerosp. Sci.* **76** 1
- [19] Miró F M et al 2019 *AIAA J.* **57** 1567
- [20] Tang H W et al 2020 *Phys. Fluids* **32** 053605
- [21] Yang H, Liang H and Zhao G 2021 *P I Mech. Eng. I-J. Sys.* **235** 563
- [22] Yates H B et al 2020 *AIAA J.* **58** 2093
- [23] Stetson K 1983 Nosetip bluntness effects on cone frustum boundary layer transition in hypersonic flow *16th Fluid and Plasmadynamics Conf. (Danvers)* (AIAA)
- [24] Kosinov A D, Maslov A A and Semionov N V 1996 Modified method of experimental study of supersonic boundary layer receptivity ed A M Kharitonov *Proc. of the Int. Conf. on the Methods of Aerophysical Research* (Springer)
- [25] Maslov A A et al 2001 *J. Fluid Mech.* **426** 73
- [26] Casper K M, Beresh S J and Schneider S P 2014 *J. Fluid Mech.* **756** 1058
- [27] Yates H et al 2018 Plasma-actuated flow control of hypersonic crossflow-induced boundary-layer transition in a Mach-6 quiet tunnel *2018 AIAA Aerospace Sciences Meeting (Kissimmee, FL)* (AIAA)
- [28] Zhang Y C, Li C and Lee C B 2020 *Phys. Fluids* **32** 071702
- [29] Li C, Zhang Y C and Lee C B 2020 *Phys. Fluids* **32** 051701
- [30] Roth J R, Sherman D M and Wilkinson S P 2000 *AIAA J.* **38** 1166
- [31] Xiong Y et al 2020 *AIAA J.* **58** 5254
- [32] Tao Y et al 2021 *Chinese J. Aeronaut.* **34** 17
- [33] Yang H S et al 2021 *Plasma Sci. Technol.* **23** 115502
- [34] Tang B L et al 2020 *Acta Phys. Sin.* **69** 155201
- [35] Stetson K and Kimmel R 1992 On hypersonic boundary-layer stability *30th Aerospace Sciences Meeting and Exhibit (Reno)* (AIAA)
- [36] Mack L M 1984 Boundary-layer linear stability theory *AGARD Report* 709
- [37] Yang H et al 2020 *Acta Aeronaut. Astronaut. Sin.* **41** 623319 (in Chinese)
- [38] Tang M X et al 2022 *J. Fluid Mech.* **931** A16
- [39] Sun Q et al 2014 *Phys. Lett. A* **378** 2672
- [40] Adam P H and Hornung H G 1997 *J. Spacecraft Rockets* **34** 614
- [41] Fedorov A et al 2015 *AIAA J.* **53** 2512
- [42] Xie L K et al 2019 *Sens. Actuators A Phys.* **297** 111550
- [43] Soudakov V G, Fedorov A V and Egorov I V 2015 *Prog. Flight Phys.* **7** 569
- [44] Zhang X et al 2020 *Plasma Sources Sci. Technol.* **29** 015017
- [45] Zhang X, Zhao Y G and Yang C 2022 *Chinese J. Aeronaut.* accepted (<https://doi.org/10.1016/j.cja.2022.01.026>)
- [46] Fedorov A 2011 *Annu. Rev. Fluid Mech.* **43** 79
- [47] Tirumala R et al 2014 *J. Phys. D: Appl. Phys.* **47** 255203